JOURNAL OF GUIDANCE, CONTROL, AND DYNAMICS
Vol. 33, No. 3, May–June 2010

Simplified Model of a Flux-Pinned Spacecraft Formation

Michael C. Norman* and Mason A. Peck†
Cornell University, Ithaca, New York 14853

DOI: 10.2514/1.46415

Spacecraft formations typically have to rely upon active control methods to maintain stable configurations. This requirement imposes an associated cost on the satellite through fuel expenditure, actuator mass, and computation time for the controller. This paper proposes using the flux-pinning interaction between a high-temperature superconductor and a magnetic field as a means to reduce these costs by passively stabilizing the dynamics governing the relative motion between spacecraft. A simplified model of a flux-pinned spacecraft formation is developed to provide the framework for future analysis. Linearization of this model about an equilibrium state allows for the development of a state-feedback control law. This framework is then applied to a simplified two-spacecraft formation in a nominally circular orbit about a central body and controlled to two distinct equilibrium separations.

Nomenclature

A	=	state matrix of linearized system
B	=	input matrix of linearized system
$\mathcal{B}$	=	frame in which the unit vectors $\mathbf{b}_1$, $\mathbf{b}_2$, and $\mathbf{b}_3$ are fixed
C	=	linear damping coefficient of $\dot{\rho}$
d_0	=	field-cooled separation between magnetic dipole and high-temperature superconductor surface
$\mathbf{F}_i$	=	generalized active force associated with ith partial velocities
$\mathbf{F}_i^*$	=	generalized inertia force associated with ith partial velocities
$f(\rho, \dot{\rho})$	=	internal forcing between two spacecraft acting along $\mathbf{b}_1$
K	=	linear quadratic regulator controller gain matrix
m_i	=	mass of ith spacecraft
$\mathcal{N}$	=	inertial frame
P_i	=	center of mass of ith spacecraft
q_i	=	ith generalized coordinate
$\mathbf{R}_i$	=	resultant of forces applied to ith spacecraft
$\mathcal{RSW}$	=	frame rotating with the formation center of mass with fixed unit vectors $\mathbf{r}$, $\mathbf{s}$, and $\mathbf{w}$
r_{cm}	=	distance between formation center of mass and central body
r_i	=	distance between P_i and central body
u_i	=	ith generalized speed
$\mathbf{v}_i^{P_j}$	=	ith partial velocity of P_j in $\mathcal{N}$
δ_i	=	radius of ith spacecraft
θ_1	=	angle between unit vector $\hat{\mathbf{s}}$ and $\mathbf{b}_2$ about $\hat{\mathbf{w}}$
θ_2	=	angle between unit vector $\hat{\mathbf{w}}$ and $\mathbf{b}_3$ about $\mathbf{b}_1$
μ	=	standard gravitational parameter for the central body
μ_{FP}	=	magnetic moment of dipole in a flux-pinning connection
μ_0	=	permeability of free space
ρ_i	=	distance between ith spacecraft's center of mass, P_i, to the formation center of mass
Ω	=	orbital mean motion of the center of mass on a circular orbit about central body
$\boldsymbol{\omega}$	=	angular velocity vector of $\mathcal{B}$ with respect to $\mathcal{RSW}$

Received 20 July 2009; revision received 25 September 2009; accepted for publication 25 October 2009.

*Graduate Research Assistant, Department of Mechanical and Aerospace Engineering, 127 Upson Hall. Student Member AIAA.

†Assistant Professor, Department of Mechanical and Aerospace Engineering, 212 Upson Hall. Member AIAA.

I. Introduction

BY DIVIDING a task between spatially separated modules, a given mission stands to obtain increased performance and mission life span. The concept of using formations to affect these gains has already found use in applications ranging from urban search-and-rescue operations to space-based observational platforms. Employing several robotic agents in a search-and-rescue operation not only increases the observational capacity of the operation but also has demonstrated an increase in human performance and communication, suggesting a hybrid team of humans and multiple vehicles coordinating to complete the task [1]. One of the more prominent examples of a planned space-based formation is that of the Terrestrial Planet Finder (TPF). The TPF aims to create an effective observational platform by combining data from several spacecraft in formation to synthesize an image that would otherwise require a much larger monolithic spacecraft to collect [2]. The Defense Advanced Research Projects Agency F6 program has further enhanced the interest and visibility of spacecraft formations by encouraging research in areas such as communication networking, close- and long-range formation flight, and collision avoidance in formation flight [3]. Spacecraft formations also introduce opportunities for modularization and reduced total system weight through the removal of mechanical linkages. These advantages, in turn, likely reduce launch costs, extend system life, and simplify component repair procedures.

One of the specific challenges that spacecraft formation flight poses is that of relative motion control. Gravitational and environmental effects tend to disperse uncontrolled and dynamically unlinked spacecraft, requiring either a control input to the system or additional dynamics linking the states of the vehicles together in a manner to maintain formation integrity. Specific solutions to the control aspect of this problem focus on the development of state-feedback controllers based on model linearization or suitable nonlinear controls schemes [4–8]. Most of these solutions require constant or periodic actuation of the system, translating into an increased mission cost through fuel expenditure and computational time. These penalties suggest instead the addition of dynamics to the system to create the desired formation. Most of the concepts in this area focus on using electromagnetic effects to couple the states of spatially separated spacecraft together, effectively adding dynamics to the system without requiring a physical linkage between the vehicles. One concept proposes the creation of a virtual coulomb structure in which each spacecraft is given a charge, resulting in electrostatic attraction and repulsion [9]. Another similar concept focuses on electrically charged spacecraft formations in orbit about a central body with a magnetic field [10]. In this case, the vehicles use

the Lorentz force to change their orbital velocity to match that of the formation. The attraction between electromagnets has also been studied for application to long-range formation flight [11]. Although these solutions do add dynamics to the system to create a multivehicle formation, Earnshaw's Theorem still requires active control of any electromagnetically interacting system attempting to maintain relative position or follow an arbitrary path [12]. As a result, a controller still needs to be developed to regulate the formation shape in these solutions.

The flux-pinning effect that occurs between a magnetic field and a high-temperature superconductor (HTSC) sidesteps this issue by instead being characterized by the change of magnetic flux through the HTSC surface rather than straight electromagnetic attraction, making it an attractive candidate for creating static connections between spacecraft or complete noncontacting kinematic mechanisms [13,14]. Although the dependence of a flux-pinned interface upon the change in magnetic flux through a surface places limitations on the effective range of the connection, many formation tasks, such as docking, are based on the close proximity of the relevant vehicle. To analyze a formation tied together with flux-pinning interfaces, we first need to adopt an appropriate mathematical model of the interaction and integrate it with a dynamics model of the formation.

II. Model Setup

Flux pinning refers to the interaction between a magnetic field and an HTSC. Motion of the magnetic field induces current vortices inside the HTSC, which then react to changes in the magnetic flux passing through the HTSC surface and establish passively stable relative separation and attitude between the HTSC and magnetic field source. The electrical resistance within the HTSC is negligible under appropriate temperature conditions, and so these vortices persist for extended periods of time. Creating an accurate physics-based model of this interaction between these vortices and the original magnetic field represents a dauntingly complex task. Several groups have worked on creating models based on approximations or around specific setups [15–19]. Kordyuk proposed a particularly general model of the flux-pinning effect termed the frozen image model. This model approximates the magnetic field due to sources inside the HTSC as the sum of two fields based on the current relative position and the field-cooled relative position of the field with respect to the HTSC surface [20].

Figure 1 describes the general setup of the image model for this analysis. Two assumptions serve to simplify the forcing model: that the magnetic dipole vector is parallel to one pointing between the centers of mass P_1 and P_2 of the spacecraft and that the force applied over the minimal separation distance between the spacecraft surfaces removes any torque interactions due to flux pinning. Furthermore, assuming spherical spacecraft of radii δ_1 and δ_2 with uniform mass distributions allows for a simple determination of the separation between the magnetic dipole and HTSC surface. As neither gravity nor flux pinning will result in a torque applied to the individual spacecraft, the attitudes of the two spacecraft will not vary. This reduces the number of states for consideration while still allowing some fidelity in the dynamics governing the relative separation between the vehicles. Although not examined explicitly in the context of orbiting bodies, experimental observations by Shoer and Peck demonstrate effectively rotational stiffness and damping between a flux-pinned HTSC and magnetic dipole pair for small angle perturbations, implying inherent disturbance rejection capabilities and passive attitude stability for appropriate separation distances [13].

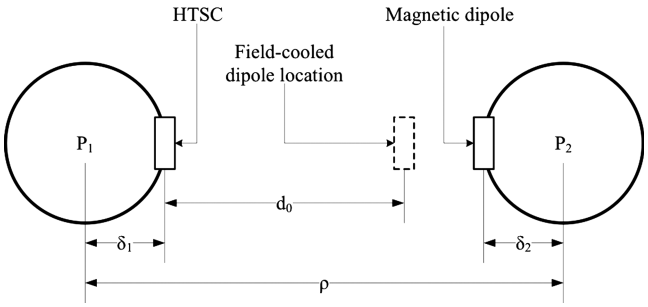

Fig. 1 Depiction of the relevant distances associated with the simplified image model. The force is assumed to always act along a vector pointing between P_1 and P_2 and produce no internal torques between the spacecraft.

The internal force produced by flux pinning under the image model depends upon the field-cooled separation d_0 of the setup: the distance between the magnetic field source and the HTSC when the HTSC is initially chilled to its superconducting state. The damping associated with flux pinning depends upon the HTSC properties and can be modified to some extent by introducing eddy current damping by placing some aluminum near the HTSC. Shoer and Peck observed that, in cases in which the magnetic field source and HTSC remain in the vicinity of their field-cooled locations, the damping due to flux pinning is approximately linear [13]. With the separation between P_1 and P_2 described as ρ, a simplified version of Kordyuk's image model with damping takes the following form:

$$f(\rho,\dot{\rho}) = \frac{3\mu_0\mu_{\mathrm{FP}}^2}{2\pi}\left(\frac{1}{(\rho-\delta_1-\delta_2+d_0)^4} - \frac{1}{16(\rho-\delta_1-\delta_2)^4}\right) + C\dot{\rho} \tag{1}$$

It should be noted that using an adapted version of Kordyuk's image model comes with the inherent assumptions of a flat, ideal superconductor and that the field penetration depth is much less than the system's characteristic dimension [20]. These assumptions place some effective limitations on the separation distances for a dipole and superconductor pair over which this force model would be a valid approximation. As the force rapidly decreases with increased separation between the HTSC surface and the dipole, flux pinning would only be appropriate for extremely close-range applications. Shoer and Peck demonstrate this model's viability for their experimental setup for separations up to 10 cm [13].

III. Relative Motion Formulation

We are interested in examining the dynamics of a flux-pinned connection between vehicles in orbit. Developing a set of equations of motion describing the relative motion of two spherical spacecraft in near-circular orbits is the first step toward analyzing the stability of this simple setup and forms the basis for examining the properties of systems of greater complexity.

Under the assumption that the formation center of mass travels on a circular orbit, we need three generalized coordinates to capture the relative motion of P_1 and P_2. Coordinates ρ, θ_1, and θ_2, as shown in Fig. 2, completely and uniquely describe the range of possible configurations of the system where θ_1 and $-\theta_2$ constitute a 3-2 Euler angle sequence:

$$q = \begin{bmatrix} q_1 \\ q_2 \\ q_3 \end{bmatrix} = \begin{bmatrix} \theta_1 \\ \theta_2 \\ \rho \end{bmatrix} \tag{2}$$

This same circular orbit assumption defines the angular velocity of frame $\mathcal{RSW}$ relative to the inertial frame $\mathcal{N}$ as a vector with constant magnitude Ω and direction $\mathbf{w}$. We choose generalized speeds as the vector measures of the inertial time derivative of the vector $\boldsymbol{\rho}$ pointing between P_1 and P_2 in terms of $\mathbf{b}_1$, $\mathbf{b}_2$, and $\mathbf{b}_3$.

$$\begin{bmatrix} u_1 \\ u_2 \\ u_3 \end{bmatrix} = \begin{bmatrix} 0 & 0 & 1 \\ c_2 q_3 & 0 & 0 \\ 0 & q_3 & 0 \end{bmatrix} \begin{bmatrix} \dot{q}_1 \\ \dot{q}_2 \\ \dot{q}_3 \end{bmatrix} + \begin{bmatrix} 0 \\ \Omega c_2 q_3 \\ 0 \end{bmatrix} \tag{3}$$

where $c_2 = \cos q_2$. Solving for the time derivative of the generalized coordinates,

$$\begin{bmatrix} \dot{q}_1 \\ \dot{q}_2 \\ \dot{q}_3 \end{bmatrix} = \begin{bmatrix} 0 & 1/c_2 q_3 & 0 \\ 0 & 0 & 1/q_3 \\ 1 & 0 & 0 \end{bmatrix} \begin{bmatrix} u_1 \\ u_2 \\ u_3 \end{bmatrix} - \begin{bmatrix} \Omega \\ 0 \\ 0 \end{bmatrix} \tag{4}$$

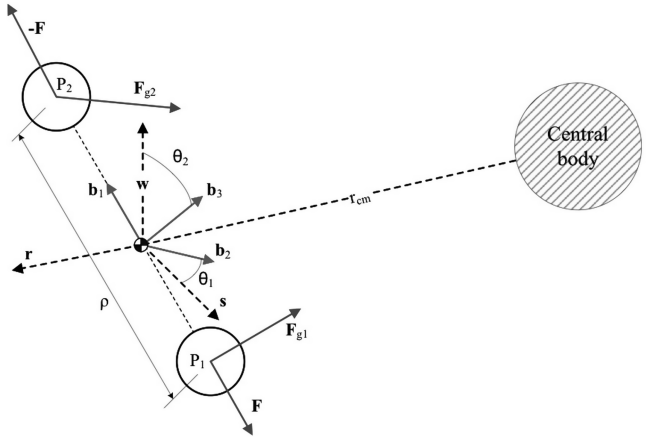

Fig. 2 Layout of the system modeled. ρ, θ_1, and θ_2 describe the configuration of the system relative to the system center of mass, assumed to travel on a circular orbit.

The two spacecraft considered in this analysis are under the influence of gravitational attraction to a central body and an internal force acting between the two vehicles. With the choice of generalized coordinates and speeds from Eqs. (2) and (3), applying these forces to the system results in the following equations of motion:

$$\dot{u}_1 = \frac{1}{q_3}(u_2^2 + u_3^2) - \mu\left(r_{\mathrm{cm}} c_1 c_2 \left(\frac{1}{r_2^3} - \frac{1}{r_1^3}\right) + \frac{q_3}{M}\left(\frac{m_1}{r_2^3} + \frac{m_2}{r_1^3}\right)\right) - \frac{M}{m_1 m_2} f(q, u) \tag{5}$$

$$\dot{u}_2 = -\frac{1}{q_3}(u_1 - t_2 u_3)u_2 + \mu r_{\mathrm{cm}} s_1 \left(\frac{1}{r_2^3} - \frac{1}{r_1^3}\right) \tag{6}$$

$$\dot{u}_3 = -\frac{1}{q_3}(u_1 u_3 + t_2 u_2^2) + \mu r_{\mathrm{cm}} c_1 s_2 \left(\frac{1}{r_2^3} - \frac{1}{r_1^3}\right) \tag{7}$$

where $c_1 = \cos q_1$, $t_2 = \tan q_2$, $M = m_1 + m_2$, r_{cm} is the constant radius of the formation center of mass' orbit, and r_1 and r_2 are functions of the generalized coordinates that describe the scalar radial distance of P_1 and P_2 to the central body. The Appendix goes into further derivation of Eqs. (5–7). Together, Eqs. (4–7) fully describe the nonlinear dynamics of the model. These equations depend upon the system conforming to the assumptions inherent in the flux-pinning model and the magnetic dipole having a negligible interaction with the ambient magnetic field. It should be noted that the representation of the equations of motion are dependent upon the variables chosen. Although an alternate set of equations may have more compact representations, our choice of u_1, u_2, and u_3 intuitively provide insight into the motion of the separation vector relative to a frame rotating with the formation in terms of Cartesian coordinates.

IV. Linearized System

The effects of the gravity gradient torque applied across the two spacecraft establishes an equilibrium orientation of the formation and in tandem with the intervehicle force **F** defines an equilibrium separation distance. These conditions correspond to the following nominal generalized coordinates and speeds:

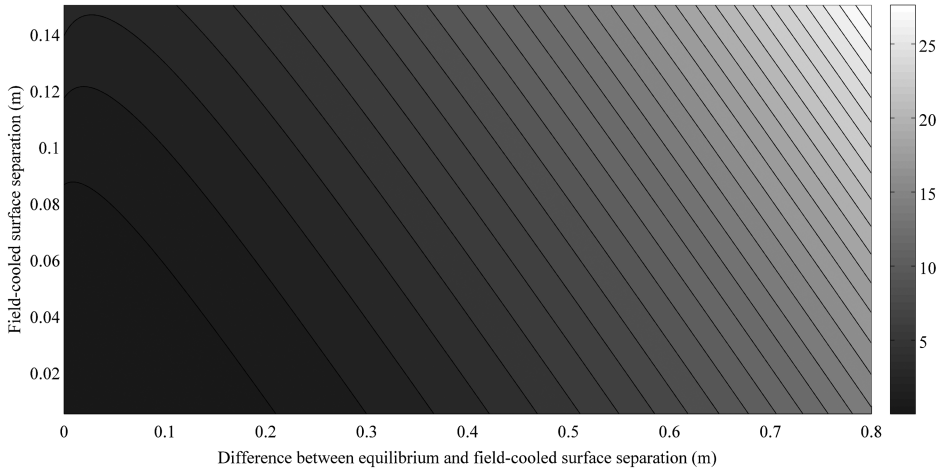

Fig. 3 $\bar{\mu}_{\mathrm{FP}}$ (J/T) required to establish a given equilibrium separation with a given field-cooled HTSC-dipole separation d_0.

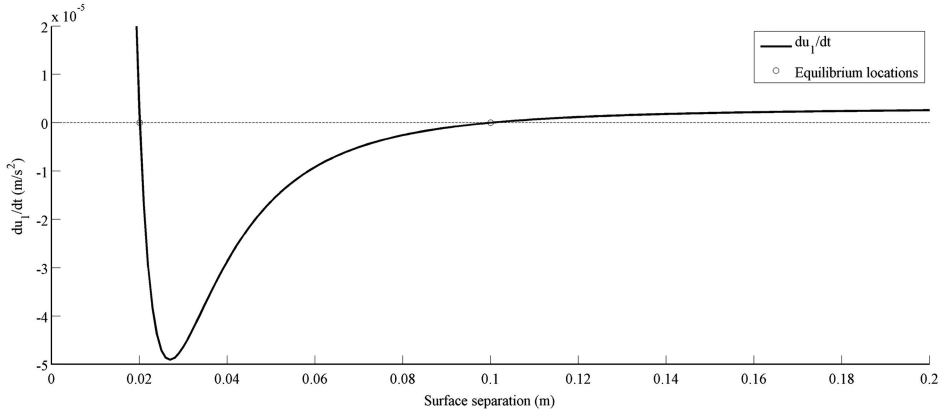

Fig. 4 Finding the zeros of $\dot{u}_1$ defines the equilibrium separation distances for a particular setup. Note the horizontal axis is in terms of surface separation, $\rho - \delta_1 - \delta_2$. In this case, using the parameters from Table 1 locates the equilibrium separation between P_1 and P_2 at distances of 0.6201 and 0.7000 m.

Table 1 Example parameters for linearization and simulation

Parameter	m_1	m_2	δ_1	δ_2	d_0	μ_{FP}	C	Orbit altitude
	100 kg	100 kg	0.3 m	0.3 m	0.02 m	0.2212 J/T	1 N s/m	600 km

$$\bar{q} = \begin{bmatrix} \bar{q}_1 \\ \bar{q}_2 \\ \bar{q}_3 \end{bmatrix} = \begin{bmatrix} 0 \\ 0 \\ \rho_0 \end{bmatrix} \quad \text{and} \quad \bar{u} = \begin{bmatrix} \bar{u}_1 \\ \bar{u}_2 \\ \bar{u}_3 \end{bmatrix} = \begin{bmatrix} 0 \\ \Omega\rho_0 \\ 0 \end{bmatrix} \tag{8}$$

which, in combination with setting $\dot{\bar{q}} = 0$ and $\dot{\bar{u}} = 0$ as required for an equilibrium and a nominal dipole moment $\bar{\mu}_{\mathrm{FP}}$, satisfy Eqs. (5–7). Considering perturbations to the state q^*, and u^*, and to the control input μ^*_{FP} from the solution $\bar{q}$, $\bar{u}$, and $\bar{\mu}_{\mathrm{FP}}$, we can form the linearized equations of motion about the equilibrium point based on Eq. (A33):

$$\begin{aligned}
\dot{q}_1^* &= \frac{1}{\rho_0}u_2^* - \frac{\Omega}{\rho_0}q_3^* \qquad \dot{q}_2^* = \frac{1}{\rho_0}u_3^* \qquad \dot{q}_3^* = u_1^* \\
\dot{u}_1^* &= \left(\frac{\mu}{M}\left(3r_{\mathrm{cm}}^2\left(\frac{m_1}{\bar{r}_2^5} + \frac{m_2}{\bar{r}_1^5}\right) + \frac{m_1}{\bar{r}_2^3}\left(1 + 3\left(\frac{m_1\rho_0}{M\bar{r}_2}\right)^2\right)\right.\right. \\
&\quad \left.\left. + \frac{m_2}{\bar{r}_1^3}\left(1 + 3\left(\frac{m_2\rho_0}{M\bar{r}_1}\right)^2\right)\right) - \Omega^2 - \frac{M}{m_1m_2}\frac{\partial f}{\partial q_3}\right)q_3^* \\
&\quad - \frac{M}{m_1m_2}Cu_1^* + 2\Omega u_2^* - \frac{3M\mu_0\bar{\mu}_{\mathrm{FP}}}{m_1m_2\pi}\left(\frac{1}{(\rho_0 - \delta_1 - \delta_2 + d_0)^4}\right. \\
&\quad \left. - \frac{1}{16(\rho_0 - \delta_1 - \delta_2)^4}\right)\mu^*_{\mathrm{FP}} \\
\dot{u}_2^* &= \mu r_{\mathrm{cm}}\left(\frac{1}{\bar{r}_2^3} - \frac{1}{\bar{r}_1^3}\right)q_1^* - \Omega u_2^* \\
\dot{u}_3^* &= \left(\mu r_{\mathrm{cm}}\left(\frac{1}{\bar{r}_2^3} - \frac{1}{\bar{r}_1^3}\right) - \Omega^2\rho_0\right)q_2^*
\end{aligned} \tag{9}$$

Setting the time derivatives of the generalized coordinates and speeds to zero in Eqs. (3) and (5–7) produces a set of equations that define states of equilibrium about which a linearization of the system can occur. Setting the angles θ_1 and θ_2 to zero as in Eq. (8) corresponds to a gravity gradient stabilized orientation of the formation and satisfies the equilibrium condition for Eqs. (6) and (7). However, substituting these values into Eq. (5) reveals that there is potentially more than one equilibrium separation distance between the two vehicles in orbit. This result arises from the flux-pinning interaction working in tandem with the effect of gravitational attraction to the central body. It should be noted that these equilibrium locations strongly depend upon the system satisfying the assumptions of Kordyuk's image model [20]. Figure 3 graphs the $\bar{\mu}_{\mathrm{FP}}$ required to establish a given surface separation and field-cooled separation between the HTSC and dipole. The zero crossings of Fig. 4 are the equilibrium separation distances in a specific case corresponding to the parameters in Table 1.

V. Simulation and Control

One possible use of the linearized model described in the previous section is the development of a state-feedback controller. Continuing to use the parameters from Table 1 and linearizing about an equilibrium state associated with a nominal separation distance found from Fig. 4 creates a state-space model of the linearized system. Applying linear quadratic regulator control synthesis to this linear system creates a basic linear state-feedback control law of the form

$$\mu_{\mathrm{FP}} = -K\begin{bmatrix} q^* \\ u^* \end{bmatrix} + \bar{\mu}_{\mathrm{FP}} \tag{10}$$

where $\bar{\mu}_{\mathrm{FP}}$ is the input required to establish the desired equilibrium separation. This constant input could be provided by either a permanent magnet or electromagnetic source.

Figure 5 depicts the separation time history of the two spacecraft described by the parameters in Table 1 resulting from an initial displacement from the equilibrium state both with and without a state-feedback controller. In this case, the desired equilibrium state corresponds to

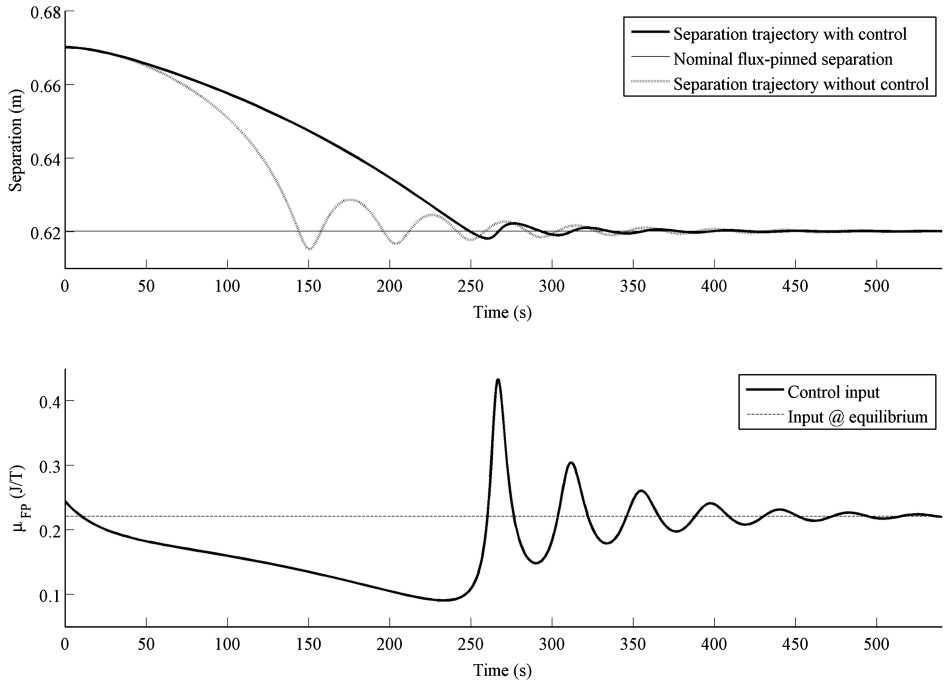

Fig. 5 Time history of the separation distance between P_1 and P_2 given the parameters described in Table 1 for both an uncontrolled and state-feedback-controlled response to the same initial condition: a) separation time history between P_1 and P_2, and b) control input time history of μ_{FP}. The desired equilibrium state is described in Eq. (11).

Table 2 Sample linear system eigenvalues about marginally stable equilibrium

A	$A - BK$
$-3.379 \cdot 10^{-10} + 0.001876i$	$-5.826 \cdot 10^{-9} + 0.001876i$
$-3.379 \cdot 10^{-10} - 0.001876i$	$-5.826 \cdot 10^{-9} - 0.001876i$
$-.001000 + 0.1483i$	$-0.01443 + 0.1479i$
$-.001000 - 0.1483i$	$-0.01443 - 0.1479i$
$0 + 0.002166i$	$0 + 0.002166i$
$0 - 0.002166i$	$0 - 0.002166i$

Table 3 Sample linear system eigenvalues about unstable equilibrium state

A	$A - BK$
$-0.02336 + 0i$	$-0.02486 + 0.009544i$
$0.003403 + 0i$	$-0.02486 - 0.009544i$
$-1.988 \cdot 10^{-5} + 0.001920i$	$-6.144 \cdot 10^{-6} + 0.001877i$
$-1.988 \cdot 10^{-5} - 0.001920i$	$-6.144 \cdot 10^{-6} - 0.001877i$
$0 + 0.002166i$	$0 + 0.002166i$
$0 - 0.002166i$	$0 - 0.002166i$

$$\bar{q} = \begin{bmatrix} 0.0 \text{ rad} \\ 0.0 \text{ rad} \\ 0.6201 \text{ m} \end{bmatrix}, \qquad \bar{u} = \begin{bmatrix} 0.0 \\ 0.0006717 \\ 0.0 \end{bmatrix} \text{ m/s}$$

$$\text{and} \quad \bar{\mu}_{\text{FP}} = 0.2212 \text{ J/T} \tag{11}$$

and the control law chosen corresponding to the gain matrix K in Eq. (10) is

$$K = [0.003317 \quad 0.0 \quad -0.4607 \quad -435.4 \quad -0.03819 \quad 0.0] \tag{12}$$

The large term corresponding to the perturbation u_1^* effectively adds damping to the system, reducing the frequency of the oscillations compared to the uncontrolled case. Examining the eigenvalues of the A matrix defined in Eq. (A33) and of $A - BK$ for the controlled system determines the stability of the linearized dynamics. The eigenvalues for the uncontrolled and state-feedback-controlled systems linearized about Eq. (11) and the gain matrix K from Eq. (12) are given in Table 2. The lack of positive real components of the eigenvalues for either A or $A - BK$ in Table 2 indicates that neither linear system is unstable. The final two eigenvalues with real components equal to zero, however, imply marginal stability for the linear system, which leaves the overall stability of the nonlinear system undetermined. The modes associated with these eigenvalues correspond to the out-of-plane motions of the system described by the θ_2 coordinate and its time derivative, $\dot{\theta}_2$, which are known to act similarly to a simple harmonic oscillator in the absence of perturbations.

The second equilibrium point found in Fig. 4 represents an opportunity to command the system in such a way as to maintain a separation distance significantly farther away than the nominal flux-pinned separation. In this specific case, the second equilibrium state corresponds to

$$\bar{q} = \begin{bmatrix} 0.0 \text{ rad} \\ 0.0 \text{ rad} \\ 0.7000 \text{ m} \end{bmatrix}, \qquad \bar{u} = \begin{bmatrix} 0.0 \\ 0.0007583 \\ 0.0 \end{bmatrix} \text{ m/s}$$

$$\text{and} \quad \bar{\mu}_{\text{FP}} = 0.2212 \text{ J/T} \tag{13}$$

Linearizing about this equilibrium state, we can again develop a state-feedback control law:

$$K = [0.1277 \quad 0.0 \quad -35.47 \quad -1097 \quad -97.37 \quad 0.0] \tag{14}$$

Table 3 lists the eigenvalues of the controlled and uncontrolled linear system about this equilibrium state. The positive real component of one of the eigenvalues of the uncontrolled system indicates that, without control, the system is unstable. This eigenvalue is associated with a combined motion of ρ and θ_1. In the controlled system, however, we see that none of the eigenvalues have positive real components, again implying marginal stability.

Figure 6 depicts a sample time history of ρ with and without the controller responding to nonequilibrium initial conditions. With the state-feedback control, the system reaches the nominal desired equilibrium value. Without it, however, the system drifts away from the prescribed equilibrium separation, as predicted in the eigenvalues of Table 3.

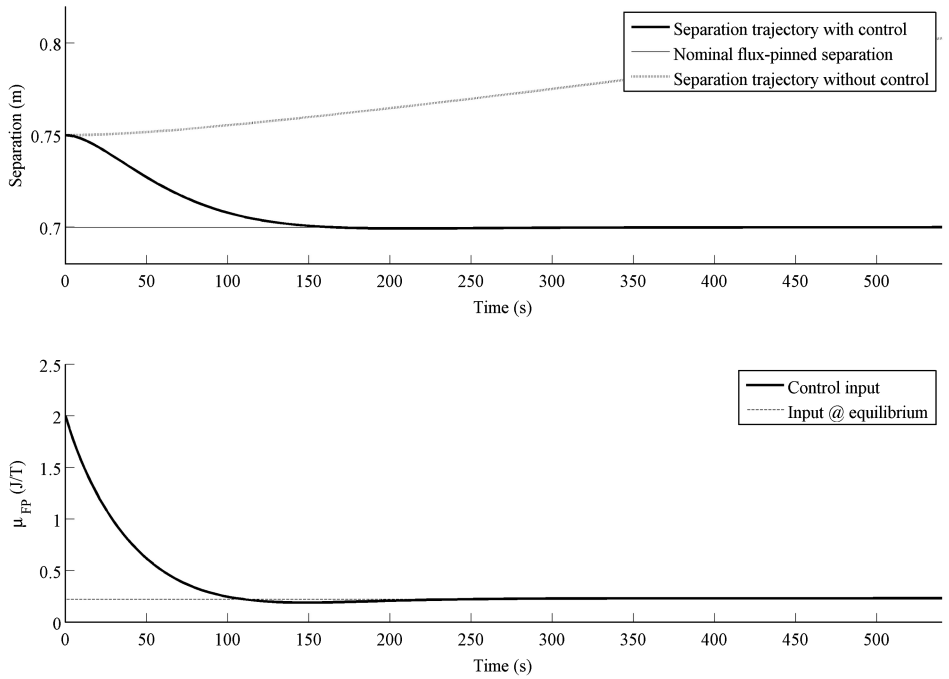

Fig. 6 Time history of the separation distance between P_1 and P_2 given the parameters described in Table 1 for both an uncontrolled and state-feedback-controlled response to the same initial condition: a) separation time history between P_1 and P_2, and b) control input time history of μ_{FP}. The desired equilibrium state is described in Eq. (13).

VI. Conclusions

Flux pinning has the potential to passively stabilize the relative motion of individual noncontacting components in a generalized system. To demonstrate some of the properties of a flux-pinned system, we created a simplified model of a two-craft formation in a nominally circular orbit. The flux-pinning interaction between the spacecraft in combination with the effects of gravitational attraction to a common central body establish dynamic equilibria. Although the effects of the gravity gradient torque acting across the two vehicles establish the equilibrium of the attitude states, some parameter choices describing the flux-pinning connection have the potential to establish two equilibrium separation distances.

The first equilibrium separation is typically close to the field-cooled separation and appears to be asymptotically stable with respect to the vehicle separation but marginally stable in some of the attitude motions. These stability properties are analogous to the effects of the gravity gradient torque on a rigid body. The second equilibrium separations are farther away than the field-cooled separation and appear to be unstable in the absence of control. These additional, more distant equilibria are created by the interaction between the internal force due to flux pinning and the effects of gravitational attraction on the central body. By implementing a simple linear state-feedback control law about these additional equilibrium states, we maintain separations between the vehicles greater than the field-cooled separations established with the cooling of the HTSC.

The mathematical framework developed provides a basis for modeling more complex formations and for linear analysis of this particular model. The flux-pinning forcing function used is a simplification of a complicated interaction with several active alternative descriptions with a variety of assumptions. The simplifications to our flux-pinning model effectively negate the torque interaction between the vehicles. In combination with the spherical spacecraft assumption, the lack of internal torques allows us to ignore the relative attitude between the vehicles and focus instead on the relative position of the two spacecraft. Although the uncontrolled separation trajectories simulated in the paper suggest that flux-pinned vehicles in orbit form passively stable arrangements, they do not definitively prove that to be the case.

Appendix: Derivation of Equations of Motion

The Appendix goes into a detailed formulation of both the nonlinear and linearized forms of the equations of motion for the system described earlier in the paper.

I. Equations of Motion

A. *Configuration Description*

The vector $\boldsymbol{\rho}$ that points from the center of mass of the first spacecraft, P_1, to the center of mass of the second spacecraft, P_2, lies parallel to a unit vector $\mathbf{b}_1$ pointing from the center of mass of the formation to either P_1 or P_2.

$$\boldsymbol{\rho} = \boldsymbol{\rho}_2 - \boldsymbol{\rho}_1 = \rho\mathbf{b}_1 = (\rho_1 + \rho_2)\mathbf{b}_2 \tag{A1}$$

From the definition of the formation center of mass, we can define the relation between $\boldsymbol{\rho}_1$ and $\boldsymbol{\rho}_2$:

$$m_1\boldsymbol{\rho}_1 + m_2\boldsymbol{\rho}_2 = 0 \tag{A2}$$

Combining Eqs. (A1) and (A2) relates the distance between P_1 and P_2 and the center of mass to the scalar ρ.

$$\rho_1 = \frac{m_2}{M}\rho \tag{A3}$$

$$\rho_2 = \frac{m_1}{M}\rho \tag{A4}$$

where $M = m_1 + m_2$.

A set of orthonormal basis vectors $\mathbf{b}_1$, $\mathbf{b}_2$, and $\mathbf{b}_3$ are fixed in frame $\mathcal{B}$ that rotates with the formation defined by P_1 and P_2. Similarly, the orthonormal vectors $\hat{\mathbf{r}}$, $\hat{\mathbf{s}}$, and $\hat{\mathbf{w}}$ are fixed in a frame $\mathcal{RSW}$ that rotates with the formation center of mass. The relative attitude between these two coordinate systems can be described by a direction cosine matrix using two angle measures θ_1 and θ_2:

$$\begin{bmatrix}\mathbf{b}_1\\ \mathbf{b}_2\\ \mathbf{b}_3\end{bmatrix} = \begin{bmatrix}c_1c_2 & s_1c_2 & s_2\\ -s_1 & c_1 & 0\\ -c_1s_2 & -s_1s_2 & c_2\end{bmatrix}\begin{bmatrix}\hat{\mathbf{r}}\\ \hat{\mathbf{s}}\\ \hat{\mathbf{w}}\end{bmatrix} \tag{A5}$$

where $s_i = \sin\theta_i$ and $c_i = \cos\theta_i$.

Under the assumption of the formation center of mass traveling on a circular orbit, we need three generalized coordinates to capture the relative motion of P_1 and P_2. Selecting coordinates ρ, θ_1, and θ_2 completely and uniquely describe the range of possible configurations of the system in terms of a spherical coordinate system of two angles and a length:

$$q = \begin{bmatrix}q_1\\ q_2\\ q_3\end{bmatrix} = \begin{bmatrix}\theta_1\\ \theta_2\\ \rho\end{bmatrix} \tag{A6}$$

B. *Velocity Definitions*

We can now further define the angular velocity of $\mathcal{B}$ with respect to $\mathcal{N}$ in terms of Ω, $\dot{q}_1$, $\dot{q}_2$, $\mathbf{b}_1$, $\mathbf{b}_2$, and $\mathbf{b}_3$ through use of Eq. (A5).

$$\boldsymbol{\omega} = (\Omega + \dot{q}_1)\hat{\mathbf{w}} - \dot{q}_2\mathbf{b}_2 = (\Omega + \dot{q}_1)s_2\mathbf{b}_1 - \dot{q}_2\mathbf{b}_2 + (\Omega + \dot{q}_1)c_2\mathbf{b}_3 \tag{A7}$$

The time derivative of the vector $\boldsymbol{\rho}$ in $\mathcal{B}$ has a simple form:

$$\frac{{}^{B}\mathrm{d}}{\mathrm{d}t}\boldsymbol{\rho} = \dot{q}_3\mathbf{b}_1 \tag{A8}$$

From $\boldsymbol{\omega}$ and ${}^{B}\mathrm{d}\boldsymbol{\rho}/\mathrm{d}t$, we can define the time derivative of $\boldsymbol{\rho}$ with respect to the inertial frame $\mathcal{N}$:

$$\frac{{}^{N}\mathrm{d}}{\mathrm{d}t}\boldsymbol{\rho} = \frac{{}^{B}\mathrm{d}}{\mathrm{d}t}\boldsymbol{\rho} + \boldsymbol{\omega}\times\boldsymbol{\rho} = \dot{q}_3\mathbf{b}_1 + q_3(\Omega + \dot{q}_1)c_2\mathbf{b}_2 + q_3\dot{q}_2\mathbf{b}_3 \tag{A9}$$

Following the method of equation of motion generation outlined by Kane and Levinson, a set of generalized speeds u_1, u_2, and u_3 need to be defined [21]. These scalar quantities typically represent the measure numbers of a relevant velocity vector expressed in a particular set of basis vectors. Basing the selection of u_1, u_2, and u_3 on the scalar components of ${}^{N}\mathrm{d}\boldsymbol{\rho}/\mathrm{d}t$ from Eq. (A9),

$$u = \begin{bmatrix}u_1\\ u_2\\ u_3\end{bmatrix} = Y(q)\dot{q} + Z(q) = \begin{bmatrix}0 & 0 & 1\\ c_2q_3 & 0 & 0\\ 0 & q_3 & 0\end{bmatrix}\begin{bmatrix}\dot{q}_1\\ \dot{q}_2\\ \dot{q}_3\end{bmatrix} + \begin{bmatrix}0\\ \Omega c_2q_3\\ 0\end{bmatrix} \tag{A10}$$

Equation (A10) can be inverted to solve for $\dot{q}$:

$$\dot{q} = W(q)\dot{u} + X(q) = \begin{bmatrix}0 & 1/c_2q_3 & 0\\ 0 & 0 & 1/q_3\\ 1 & 0 & 0\end{bmatrix}\begin{bmatrix}\dot{q}_1\\ \dot{q}_2\\ \dot{q}_3\end{bmatrix} - \begin{bmatrix}\Omega\\ 0\\ 0\end{bmatrix} \tag{A11}$$

Combining Eqs. (A3), (A4), (A9), and (A10) defines the velocity vectors of P_1 and P_2 relative to their center of mass in the inertial frame $\mathcal{N}$:

$$\frac{{}^{N}\mathrm{d}}{\mathrm{d}t}\boldsymbol{\rho}_1 = -\frac{m_2}{M}u_1\mathbf{b}_1 - \frac{m_2}{M}u_2\mathbf{b}_2 - \frac{m_2}{M}u_3\mathbf{b}_3 \tag{A12}$$

$$\frac{{}^{N}\mathrm{d}}{\mathrm{d}t}\boldsymbol{\rho}_2 = \frac{m_1}{M}u_1\mathbf{b}_1 + \frac{m_1}{M}u_2\mathbf{b}_2 + \frac{m_1}{M}u_3\mathbf{b}_3 \tag{A13}$$

These velocities, in turn, define the partial velocities of P_1 and P_2 in $\mathcal{N}$.

$$\begin{aligned} \mathbf{v}_1^{P1} &= -\frac{m_2}{M}\mathbf{b}_1 \qquad \mathbf{v}_2^{P1} = -\frac{m_2}{M}\mathbf{b}_2 \qquad \mathbf{v}_3^{P1} = -\frac{m_2}{M}\mathbf{b}_3 \\ \mathbf{v}_1^{P2} &= \frac{m_1}{M}\mathbf{b}_1 \qquad \mathbf{v}_2^{P2} = \frac{m_1}{M}\mathbf{b}_2 \qquad \mathbf{v}_3^{P2} = \frac{m_1}{M}\mathbf{b}_3 \end{aligned} \tag{A14}$$

C. Generalized Inertia Forces

From Kane and Levinson, the equations of motion of a system are the sum of the generalized inertia forces and generalized active forces for each of the degrees of freedom in the system [21]. For an unconstrained system with n generalized speeds and v points of interest, the generalized inertia forces take the following form:

$$F_r^* = \sum_{i=1}^{v} -m_i\mathbf{v}_r^{P_i}\cdot\mathbf{a}_i = -\frac{1}{2}\sum_{i=1}^{v} m_i \sum_{j=1}^{n}\left(\frac{\mathrm{d}}{\mathrm{d}t}\frac{\partial}{\partial\dot{q}_j}\mathbf{v}_i^2 - \frac{\partial}{\partial q_j}\mathbf{v}_i^2\right)W_{\mathrm{jr}} \quad \text{for } r = 1\ldots n \tag{A15}$$

where $\mathbf{v}_i^2$ is the square of the norm of the velocity of P_i, $\mathbf{a}_i$ is the acceleration of P_i, and W_{jr} are elements of the matrix W describing the derivatives of the generalized coordinates in terms of the generalized speeds, as in Eq. (A11). For the generalized coordinates in Eq. (A6), generalized speeds in Eq. (A10), velocities in Eqs. (A12) and (A13), and partial velocities in Eq. (A19), the relevant partial derivatives are summed to form the generalized inertia forces of the system:

$$F_1^* = -\frac{m_1m_2}{M}\left(\dot{u}_1 - \frac{1}{q_3}(u_2^2 + u_3^2)\right) \tag{A16}$$

$$F_2^* = -\frac{m_1m_2}{M}\left(\dot{u}_2 + \frac{1}{q_3}(u_1 - t_2u_3)u_2\right) \tag{A17}$$

$$F_3^* = -\frac{m_1m_2}{M}\left(\dot{u}_3 + \frac{1}{q_3}(u_1u_3 + t_2u_2^2)\right) \tag{A18}$$

where $t_2 = \tan q_2$.

D. Generalized Active Forces

The generalized active forces associated with a particular generalized speed are the sum of the dot products between force resultants and appropriate partial velocities over all bodies:

$$F_r = \sum_{i=1}^{v}\mathbf{v}_r^{P_i}\cdot\mathbf{R}_i \tag{A19}$$

The resultants $\mathbf{R}_1, \mathbf{R}_2$ are the sum of all forces applied to P_1 and P_2, respectively. In this formulation, these include gravitation ($\mathbf{F}_g$) and the intersatellite force ($\mathbf{F}$). The gravitational force applied to P_1 can be represented in terms of the generalized coordinates q and constants:

$$\mathbf{F}_{g1} = -\frac{\mu m_1}{r_1^3}\mathbf{r}_1 = -\mu m_1\left(\left(r_{\mathrm{cm}}c_1c_2 - \frac{m_2}{M}q_3\right)\mathbf{b}_1 - r_{\mathrm{cm}}s_1\mathbf{b}_2 - r_{\mathrm{cm}}c_1s_2\mathbf{b}_3\right)\frac{1}{r_1^3} \tag{A20}$$

where $r_1 = (r_{\mathrm{cm}}^2 - 2r_{\mathrm{cm}}\frac{m_2}{M}c_1c_2q_3 + (\frac{m_2}{M}q_3))^{1/2}$. Similarly, $\mathbf{F}_{g2}$ can be defined in terms of q and constants:

$$\mathbf{F}_{g2} = -\frac{\mu m_2}{r_2^3}\mathbf{r}_2 = -\mu m_2\left(\left(r_{\mathrm{cm}}c_1c_2 + \frac{m_1}{M}q_3\right)\mathbf{b}_1 - r_{\mathrm{cm}}s_1\mathbf{b}_2 - r_{\mathrm{cm}}c_1s_2\mathbf{b}_3\right)\frac{1}{r_2^3} \tag{A21}$$

where $r_2 = (r_{\mathrm{cm}}^2 + 2r_{\mathrm{cm}}\frac{m_1}{M}c_1c_2q_3 + (\frac{m_1}{M}q_3))^{1/2}$. The interspacecraft force $\mathbf{F}$ is assumed to be parallel to and applied at a point along the unit vector $\mathbf{b}_1$ pointing between P_1 and P_2.

$$\mathbf{F} = f(q,u)\mathbf{b}_1 \tag{A22}$$

These force descriptions define the resultants of P_1 and P_2:

$$\mathbf{R}_1 = \mathbf{F}_{g1} + \mathbf{F} \tag{A23}$$

$$\mathbf{R}_2 = \mathbf{F}_{g2} - \mathbf{F} \tag{A24}$$

These resultants can then be applied to Eq. (A19):

$$\mathbf{F}_1 = -\mu\frac{m_1m_2}{M}\left(r_{\mathrm{cm}}c_1c_2\left(\frac{1}{r_2^3} - \frac{1}{r_1^3}\right) + \frac{q_3}{M}\left(\frac{m_1}{r_2^3} + \frac{m_2}{r_1^3}\right)\right) - f(q,u) \tag{A25}$$

$$\mathbf{F}_2 = \mu\frac{m_1m_2}{M}r_{\mathrm{cm}}s_1\left(\frac{1}{r_2^3} - \frac{1}{r_1^3}\right) \tag{A26}$$

$$\mathbf{F}_3 = \mu\frac{m_1m_2}{M}r_{\mathrm{cm}}c_1s_2\left(\frac{1}{r_2^3} - \frac{1}{r_1^3}\right) \tag{A27}$$

E. Equations of Motion

The equations of motion associated with a particular generalized speed correspond to the sum of the appropriate generalized inertia force and generalized active force:

$$F_r^* + F_r = 0 \tag{A28}$$

where $r = 1\cdots 3$. Summing Eqs. (A16) and (A25) and solving for $\dot{u}_1$,

$$\dot{u}_1 = \frac{1}{q_3}(u_2^2 + u_3^2) - \mu\left(r_{\mathrm{cm}}c_1c_2\left(\frac{1}{r_2^3} - \frac{1}{r_1^3}\right) + \frac{q_3}{M}\left(\frac{m_1}{r_2^3} + \frac{m_2}{r_1^3}\right)\right) - \frac{M}{m_1m_2}f(q,u) \tag{A29}$$

Similarly, summing Eqs. (A17) and (A26) and solving for $\dot{u}_2$,

$$\dot{u}_2 = -\frac{1}{q_3}(u_1 - t_2u_3)u_2 + \mu r_{\mathrm{cm}}s_1\left(\frac{1}{r_2^3} - \frac{1}{r_1^3}\right) \tag{A30}$$

Finally, summing Eqs. (A18) and (A27) and solving for $\dot{u}_3$,

$$\dot{u}_3 = -\frac{1}{q_3}(u_1u_3 + t_2u_2^2) + \mu r_{\mathrm{cm}}c_1s_2\left(\frac{1}{r_2^3} - \frac{1}{r_1^3}\right) \tag{A31}$$

II. Linearization

Linearizing the nonlinear differential equations (4–7) about an appropriate equilibrium state allows us to examine the infinitesimal stability properties of the original nonlinear system and perform linear controller synthesis. Linearizing an arbitrary function g of q, u, and μ_{FP},

$$g(q,u,\mu_{\mathrm{FP}}) \approx g(\bar{q},\bar{u}) + \left.\frac{\partial g}{\partial q}\right|_0 q^* + \left.\frac{\partial g}{\partial u}\right|_0 u^* + \left.\frac{\partial g}{\partial \mu_{\mathrm{FP}}}\right|_0 \mu_{\mathrm{FP}}^* \tag{A32}$$

where $q = q^* + \bar{q}$, $u = u^* + \bar{u}$, and $\mu_{\mathrm{FP}} = \mu_{\mathrm{FP}}^* + \bar{\mu}_{\mathrm{FP}}$.

Applying Eq. (A32) to Eqs. (4–7) and arranging in a matrix format,

$$\begin{bmatrix} \dot{q}_1^* \\ \dot{q}_2^* \\ \dot{q}_3^* \\ \dot{u}_1^* \\ \dot{u}_2^* \\ \dot{u}_3^* \end{bmatrix} = \begin{bmatrix} 0 & \frac{\partial \dot{q}_1}{\partial q_2}|_0 & \frac{\partial \dot{q}_1}{\partial q_3}|_0 & 0 & \frac{\partial \dot{q}_1}{\partial u_2}|_0 & 0 \\ 0 & 0 & \frac{\partial \dot{q}_2}{\partial q_3}|_0 & 0 & 0 & \frac{\partial \dot{q}_2}{\partial u_3}|_0 \\ 0 & 0 & \frac{\partial \dot{q}_3}{\partial q_3}|_0 & 0 & 0 & 0 \\ \frac{\partial \dot{u}_1}{\partial q_1}|_0 & \frac{\partial \dot{u}_1}{\partial q_2}|_0 & \frac{\partial \dot{u}_1}{\partial q_3}|_0 & \frac{\partial \dot{u}_1}{\partial u_1}|_0 & \frac{\partial \dot{u}_1}{\partial u_2}|_0 & \frac{\partial \dot{u}_1}{\partial u_3}|_0 \\ \frac{\partial \dot{u}_2}{\partial q_1}|_0 & \frac{\partial \dot{u}_2}{\partial q_2}|_0 & \frac{\partial \dot{u}_2}{\partial q_3}|_0 & \frac{\partial \dot{u}_2}{\partial u_1}|_0 & \frac{\partial \dot{u}_2}{\partial u_2}|_0 & \frac{\partial \dot{u}_2}{\partial u_3}|_0 \\ \frac{\partial \dot{u}_3}{\partial q_1}|_0 & \frac{\partial \dot{u}_3}{\partial q_2}|_0 & \frac{\partial \dot{u}_3}{\partial q_3}|_0 & \frac{\partial \dot{u}_3}{\partial u_1}|_0 & \frac{\partial \dot{u}_3}{\partial u_2}|_0 & \frac{\partial \dot{u}_3}{\partial u_3}|_0 \end{bmatrix} \begin{bmatrix} q_1^* \\ q_2^* \\ q_3^* \\ u_1^* \\ u_2^* \\ u_3^* \end{bmatrix} + \begin{bmatrix} 0 \\ 0 \\ 0 \\ \frac{\partial \dot{u}_1}{\partial \mu_{\mathrm{FP}}}|_0 \\ 0 \\ 0 \end{bmatrix} \mu_{\mathrm{FP}}^* \tag{A33}$$

or

$$\begin{bmatrix} \dot{q}^* \\ \dot{u}^* \end{bmatrix} = A(\bar{q}, \bar{u}, \bar{\mu}_{\mathrm{FP}}) \begin{bmatrix} q^* \\ u^* \end{bmatrix} + B(\bar{q}, \bar{u}, \bar{\mu}_{\mathrm{FP}}) \mu_{\mathrm{FP}}^* \tag{A34}$$

This corresponds to a state-space representation of the linearized system. The partial derivatives from Eq. (A33) are

$$\frac{\partial \dot{q}_1}{\partial q_2} = \frac{t_2 u_2}{c_2 q_3} \qquad \frac{\partial \dot{q}_1}{\partial q_3} = -\frac{u_2}{c_2 q_3^2} \qquad \frac{\partial \dot{q}_1}{\partial u_2} = \frac{1}{c_2 q_3} \qquad \frac{\partial \dot{q}_2}{\partial q_3} = -\frac{u_3}{q_3^2} \qquad \frac{\partial \dot{q}_2}{\partial u_3} = \frac{1}{q_3} \qquad \frac{\partial \dot{q}_3}{\partial u_1} = 1$$

$$\frac{\partial \dot{u}_1}{\partial q_1} = \mu \left(r_{\mathrm{cm}} s_1 c_2 \left(\frac{1}{r_2^3} - \frac{1}{r_1^3} \right) - \left(r_{\mathrm{cm}} c_1 c_2 + \frac{m_1}{M} q_3 \right) \frac{\partial}{\partial q_1} r_2^{-3} + \left(r_{\mathrm{cm}} c_1 c_2 - \frac{m_2}{M} q_3 \right) \frac{\partial}{\partial q_1} r_1^{-3} \right)$$

$$\frac{\partial \dot{u}_1}{\partial q_2} = \mu \left(r_{\mathrm{cm}} c_1 s_2 \left(\frac{1}{r_2^3} - \frac{1}{r_1^3} \right) - \left(r_{\mathrm{cm}} c_1 c_2 + \frac{m_1}{M} q_3 \right) \frac{\partial}{\partial q_2} r_2^{-3} + \left(r_{\mathrm{cm}} c_1 c_2 - \frac{m_2}{M} q_3 \right) \frac{\partial}{\partial q_2} r_1^{-3} \right)$$

$$\frac{\partial \dot{u}_1}{\partial q_3} = -\mu \left(\left(r_{\mathrm{cm}} c_1 c_2 + \frac{m_1}{M} q_3 \right) \frac{\partial}{\partial q_3} r_2^{-3} - \left(r_{\mathrm{cm}} c_1 c_2 - \frac{m_2}{M} q_3 \right) \frac{\partial}{\partial q_3} r_1^{-3} + \frac{1}{M} \left(\frac{m_1}{r_2^3} + \frac{m_2}{r_1^3} \right) \right) - \frac{1}{q_3^2} (u_2^2 + u_3^2) + \frac{M}{m_1 m_2} \frac{\partial f}{\partial q_3}$$

$$\frac{\partial \dot{u}_1}{\partial u_1} = \frac{M}{m_1 m_2} \frac{\partial f}{\partial u_1} \qquad \frac{\partial \dot{u}_1}{\partial u_2} = \frac{2u_2}{q_3} \qquad \frac{\partial \dot{u}_1}{\partial u_3} = \frac{2u_3}{q_3}$$

$$\frac{\partial \dot{u}_2}{\partial q_1} = \mu r_{\mathrm{cm}} \left(s_1 \left(\frac{\partial}{\partial q_1} r_2^{-3} - \frac{\partial}{\partial q_1} r_1^{-3} \right) + c_2 (r_2^{-3} - r_1^{-3}) \right)$$

$$\frac{\partial \dot{u}_2}{\partial q_2} = \frac{u_2 u_3}{q_3 c_2^2} + \mu r_{\mathrm{cm}} s_1 \left(\frac{\partial}{\partial q_2} r_2^{-3} - \frac{\partial}{\partial q_2} r_1^{-3} \right)$$

$$\frac{\partial \dot{u}_2}{\partial q_3} = \frac{1}{q_3^2} (u_1 - t_2 u_3) u_2 + r_{\mathrm{cm}} s_1 \left(\frac{\partial}{\partial q_1} r_2^{-3} - \frac{\partial}{\partial q_1} r_1^{-3} \right)$$

$$\frac{\partial \dot{u}_2}{\partial u_1} = -\frac{u_2}{q_3} \qquad \frac{\partial \dot{u}_2}{\partial u_2} = \frac{1}{q_3} (t_2 u_3 - u_1) \qquad \frac{\partial \dot{u}_2}{\partial u_3} = \frac{t_2 u_2}{q_3}$$

$$\frac{\partial \dot{u}_3}{\partial q_1} = \mu r_{\mathrm{cm}} s_2 \left(c_1 \left(\frac{\partial}{\partial q_1} r_2^{-3} - \frac{\partial}{\partial q_1} r_1^{-3} \right) - s_1 (r_2^{-3} - r_1^{-3}) \right)$$

$$\frac{\partial \dot{u}_3}{\partial q_2} = -\frac{u_2^2}{q_3 c_2^2} + \mu r_{\mathrm{cm}} c_1 \left(s_2 \left(\frac{\partial}{\partial q_2} r_2^{-3} - \frac{\partial}{\partial q_2} r_1^{-3} \right) + c_2 (r_2^{-3} - r_1^{-3}) \right)$$

$$\frac{\partial \dot{u}_3}{\partial q_3} = \frac{1}{q_3} (u_1 u_3 + t_2 u_2^2) \mu r_{\mathrm{cm}} c_1 s_2 \left(\frac{\partial}{\partial q_3} r_2^{-3} - \frac{\partial}{\partial q_3} r_1^{-3} \right)$$

$$\frac{\partial \dot{u}_3}{\partial u_1} = -\frac{u_3}{q_3} \qquad \frac{\partial \dot{u}_3}{\partial u_2} = -2 \frac{t_2 u_2}{q_3} \qquad \frac{\partial \dot{u}_3}{\partial u_3} = -\frac{u_1}{q_3}$$

The preceding set of equations make use of a few extra partial derivatives:

$$\frac{\partial}{\partial q_1} r_1^{-3} = -3 \frac{m_2 r_{\mathrm{cm}}}{M r_1^5} s_1 c_2 q_3 \qquad \frac{\partial}{\partial q_1} r_2^{-3} = 3 \frac{m_1 r_{\mathrm{cm}}}{M r_2^5} s_1 c_2 q_3$$

$$\frac{\partial}{\partial q_2} r_1^{-3} = -3 \frac{m_2 r_{\mathrm{cm}}}{M r_1^5} c_1 s_2 q_3 \qquad \frac{\partial}{\partial q_2} r_2^{-3} = 3 \frac{m_1 r_{\mathrm{cm}}}{M r_2^5} c_1 s_2 q_3$$

$$\frac{\partial}{\partial q_3} r_1^{-3} = 3 \frac{m_2}{M r_1^5} \left(r_{\mathrm{cm}} c_1 c_2 + \frac{m_2}{M} q_3 \right)$$

$$\frac{\partial}{\partial q_3} r_2^{-3} = -3 \frac{m_1}{M r_2^5} \left(r_{\mathrm{cm}} c_1 c_2 - \frac{m_1}{M} q_3 \right) \qquad \frac{\partial f}{\partial u_1} = C$$

$$\frac{\partial f}{\partial q_3} = -6 \frac{\mu_0 \mu_{\mathrm{FP}}^2}{\pi} \left(\frac{1}{(q_3 - \delta_1 - \delta_2 + d_0)^5} - \frac{1}{16 (q_3 - \delta_1 - \delta_2)^5} \right)$$

$$\frac{\partial f}{\partial \mu_{\mathrm{FP}}} = 3 \frac{\mu_0 \mu_{\mathrm{FP}}}{\pi} \left(\frac{1}{(q_3 - \delta_1 - \delta_2 + d_0)^4} - \frac{1}{16 (q_3 - \delta_1 - \delta_2)^4} \right)$$

References

[1] Burke, J., and Murphy, R., "Human-Robot Interaction in USAR Technical Search: Two Heads Are Better Than One," *13th IEEE International Workshop on Robot and Human Interactive Communication*, Inst. of Electrical and Electronics Engineers, New York, Sept. 2004, pp. 307–312. doi:10.1109/ROMAN.2004.1374778

[2] Lawson, P., "The Terrestrial Planet Finder," *Aerospace Conference, 2001, IEEE Proceedings*, Vol. 4, Inst. of Electrical and Electronics Engineers, New York, 2001, pp. 2005–2011.

[3] "System F6," Defense Advanced Research Projects Agency, BAA07-31, July 2007.

[4] Zanon, D. J., and Campbell, M. E., "Optimal Planner for Spacecraft Formations in Elliptical Orbits," *Journal of Guidance, Control, and Dynamics*, Vol. 29, No. 1, Jan.–Feb. 2006, pp. 161–171. doi:10.2514/1.7236

[5] Inalhan, G., Tillerson, M., and How, J. P., "Relative Dynamics and Control of Spacecraft Formations in Eccentric Orbits," *Journal of Guidance, Control, and Dynamics*, Vol. 25, No. 1, Jan.–Feb. 2002, pp. 48–59. doi:10.2514/2.4874

[6] Ulybyshev, Y., "Long-Term Formation Keeping of Satellite Constellations Using Linear-Quadratic Controller," *Journal of Guidance, Control, and Dynamics*, Vol. 21, No. 1, Jan.–Feb. 1998, pp. 109–115. doi:10.2514/2.4204

[7] Millard, L., and Howell, K., "Control of Interferometric Spacecraft Arrays for (U, V) Plane Coverage in Multi-Body Regimes," American Astronautical Society Paper 07-153, Jan. 2007.

[8] Hamel, J.-F., and de Lafontaine, J., "Neighboring Optimum Feedback Control Law for Earth-Orbiting Formation-Flying Spacecraft," *Journal of Guidance, Control, and Dynamics*, Vol. 32, No. 1, 2009, pp. 290–299. doi:10.2514/1.32778

[9] Berryman, J., and Schaub, H., "Analytical Charge Analysis for Two-and Three-Craft Coulomb Formations," *Journal of Guidance, Control, and Dynamics*, Vol. 30, No. 6, Nov.–Dec. 2007, pp. 1701–1710. doi:10.2514/1.23785

[10] Atchison, J. A., and Peck, M. A., "A Millimeter-Scale Lorentz-Propelled Spacecraft," AIAA Paper 2007-6847, Aug. 2007.

[11] Miller, D., Sedwick, R., Kong, E., and Schweighart, S., "Electromagnetic Formation Flight for Sparse Aperture Telescopes," *Aerospace Conference Proceedings*, Vol. 2, Inst. of Electrical and Electronics Engineers, New York, 2002, pp. 2-729–2-741. doi:10.1109/AERO.2002.1035616

[12] Earnshaw, S., "On the Nature of the Molecular Forces Which Regulate the Constitution of the Luminiferous Ether," *Transactions of the Cambridge Philosophical Society*, Vol. 7, No. 1, 1842, pp. 97–112.

[13] Shoer, J., and Peck, M., "Stiffness of a Flux-Pinned Virtual Structure for Modular Spacecraft," *Journal of the British Interplanetary Society*, Vol. 62, No. 2, Feb. 2009, pp. 57–65.

[14] Shoer, J. P., and Peck, M. A., "Reconfigurable Spacecraft as Kinematic Mechanisms," *Journal of Spacecraft and Rockets*, Vol. 46, No. 2, March–April 2009, pp. 466–469. doi:10.2514/1.37641

[15] Yang, Z. J., and Hull, J. R., "Effect of Size on Levitation Force in a Magnet/Superconductor System," *Journal of Applied Physics*, Vol. 79, No. 6, 1996, pp. 3318–3322. doi:10.1063/1.361232

[16] Johansen, T. H., Mestl, H., and Bratsberg, H., "Investigation of the Lateral Magnetic Force and Stiffness Between a High-T_c Superconductor and Magnet of Rectangular Shapes," *Journal of Applied Physics*, Vol. 75, No. 3, Feb. 1994, pp. 1667–1670. doi:10.1063/1.356351

[17] Chang, P.-Z., Moon, F. C., Hull, J. R., and Mulcahy, T. M., "Levitation Force and Magnetic Stiffness in Bulk High-Temperature Superconductors," *Journal of Applied Physics*, Vol. 67, No. 9, 1990, pp. 4358–4360. doi:10.1063/1.344927. doi:

[18] Tsuchimoto, M., Kojima, T., Takeuchi, H., and Honma, T., "Numerical Analyses of Levitation Force and Flux Creep on High T_c Superconductor," *IEEE Transactions on Magnetics*, Vol. 29, No. 6, Nov. 1993, pp. 3577–3579. doi:10.1109/20.281235

[19] Hull, J. R., and Cansiz, A., "Vertical and Lateral Forces Between a Permanent Magnet and High-Temperature Superconductor," *Journal of Applied Physics*, Vol. 86, No. 11, 1999, pp. 6396–6404. doi:10.1063/1.371703

[20] Kordyuk, A. A., "Magnetic Levitation for Hard Superconductors," *Journal of Applied Physics*, Vol. 83, No. 1, Jan 1998, pp. 610–613. doi:10.1063/1.366648

[21] Kane, T. R., and Levinson, D. A., "Formulation of Equations of Motion," *Dynamics: Theory and Applications*, McGraw–Hill, New York, 1985, pp. 158–186.